IEIE Transactions on Smart Processing and Computing, vol. 5, no. 6, December 2016
https://doi.org/10.5573/IEIESPC.2016.5.6.454

Unbounded Binary Search Method for Fast-tracking Maximum Power Point of Photovoltaic Modules

Yohan Hong[1], Yong Sin Kim[2], and Kwang-Hyun Baek[1]

[1] School of Electrical and Electronics Engineering, Chung-Ang University / 84 Heukseok-Ro Dongjak-Gu, Seoul, 156-756 Korea {cmosmaster, kbaek}@cau.ac.kr
[2] School of Electrical Engineering, Korea University / 145 Anam-ro, Seongbuk-Gu, Seoul, 136-701 Korea shonkim@korea.ac.kr

* Corresponding Author: Kwang-Hyun Baek

Received October 17, 2016; Accepted December 8, 2016; Published December 30, 2016

** Regular Paper*

***Abstract*:** A maximum power point tracking (MPPT) system with fast-tracked time and high power efficiency is presented in this paper. The proposed MPPT system uses an unbounded binary search (UBS) algorithm that continuously tracks the maximum power point (MPP) with a binary system to follow the MPP under rapid–weather-change conditions. The proposed algorithm can decide the correct direction of the MPPT system while comparing the previous power point with the present power point. And then, by fixing the MPP until finding the next MPP, there is no oscillation of voltage MPP, which maximizes the overall power efficiency of the photovoltaic module. With these advantages, this proposed UBS is able to detect the MPP more effectively. This MPPT system is based on a boost converter with a micro-control unit to control analog-to-digital converters and pulse width modulation. Analysis of this work and experimental results show that the proposed UBS MPPT provides fast, accurate tracking with no oscillation in situations where weather rapidly changes and shadow is caused by all sorts of things. The tracking time is reduced by 87.3% and 66.1% under dynamic-state and steady-state operation, respectively, as compared with the conventional 7-bit perturb and observe technique.

***Keywords*: Binary search, Dc-dc converter, Fast-tracking MPP, Photovoltaic module**

1. Introduction

Recently, the growing energy demand that consumes a lot of fossil fuel, making noxious gases, has driven research and development of renewable energy sources, such as wind, rain, tide, geothermal heat, and solar. Among these sources, the electrical energy source from photovoltaic (PV) modules has seen brisk growth, and has been considered a promising energy source over the last few years because it is free, plentiful, and widely distributed over the Earth. In addition, components in PV modules can be recycled. Each PV cell in the module can be converted into a new element of a new wafer. The aluminum frames can also be recycled [10, 11]. These advantages make the PV module a future alternative electricity source. However, a PV module should be accompanied by a maximum power point tracking (MPPT) technique to maximize the efficiency of the energy system using the PV module due to non-uniform characteristics of the current-versus-voltage curve in the PV module.

These features are dependent upon variation in solar irradiation conditions and the module's temperature, which results in a change in the maximum power point (MPP). In order to maintain maximum power and to track the MPP, there has been research into making useful MPPT techniques in various ways: perturb and observe (P&O), P&O based on a power-increment-aided (PI) controller, *dP*-P&O, incremental conductance (INC), and PI-INC with two-phased tracking, a successive approximation register (SAR) method [2-7], and unbounded binary search (UBS) [1].

Among MPPT techniques mentioned, even though the P&O MPPT algorithm [2] has been mostly used until now (owing to easy implementation), the response time in the P&O method in the dynamic state is slower than other algorithms, because one step of the P&O method increases

from comparing the current power to the previous power. In the steady state, the operating point oscillates around the maximum power point. This phenomenon wastes a large amount of available energy. To minimize the fluctuation, P&O based on a PI controller was suggested [3]. This method can mitigate the oscillation by using a closed-loop control. However, because of the closed-loop control, the response time of P&O based on a PI controller is slower than other algorithms in situations where rapid weather change occurs.

In the INC algorithm, which seeks to overcome the limitations caused by P&O [5], the voltage of the PV module is always adjusted according to the MPP voltage. It is based on the incremental and instantaneous conductance of the PV module. This method makes it theoretically possible for the perturbation to be stopped. However, on the left-hand side of the MPP, the conductance response to PV voltage is even less sensitive than the right-hand side of the MPP and the point of the MPP, because the variation of current in the PV module is almost zero. On the other hand, the conductance response to PV voltage on the right-hand side of the MPP is much more sensitive, because the slope of the I-V curve of the PV module is precipitous. In order to reduce the difference in speed between the two sides, PI-INC MPPT was suggested [6]. This algorithm is carried out by using both current-versus-voltage curve and power-versus-voltage curve. Although the INC algorithm can overcome the disadvantages of the P&O algorithm, the INC algorithm increases the complexity of the hardware and software, and leads to increased computation time [12].

Another MPPT technique that can deal with the limitations of P&O and INC is the successive approximation register MPPT method [7]. This algorithm is based on the P&O algorithm with a fast MPPT time. It is also possible for this algorithm to prevent fluctuation around the MPP. The drawback of the SAR MPPT is seen when weather changes rapidly and it is cloudy. The variation in the weather causes the SAR MPPT to start finding a new MPP at the old MPP with a factor of 2 for fixed N-bit resolution. Therefore,

SAR MPPT can need more response time than P&O MPPT, and depends on arranged resolution in terms of response time.

This paper presents a UBS based on [1]. The UBS technique detects the MPP with a fast tracking time and no oscillation in a real environment. The advantage of this work can be useful in urban areas where partial shading occurs frequently, and in Northern Europe, where moving clouds are often present in the sky [5]. Also, non-fluctuation at the MPP can provide constant power efficiency during clear weather conditions and prolongs the life of the components in the MPPT controller [1]. This implementation of a revised UBS algorithm consists of a boost converter, a microcontroller, and a 6 ohm resistor load. In Section 2, characteristics of the PV panel are introduced. Section 3 describes previous algorithms. Section 4 presents the proposed UBS algorithm. In Section 5, experimental results are shown with measured data. Lastly, Section 6 offers the conclusion to the paper.

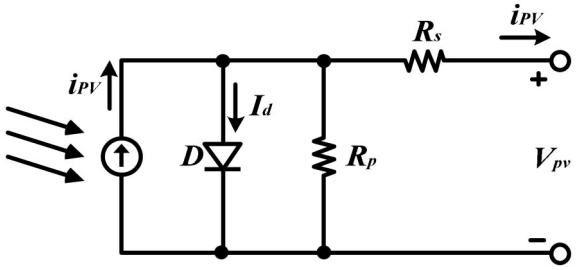

Fig. 1. The equivalent circuit of a photovoltaic cell.

2. Characteristics of PV module

A photovoltaic cell can be represented by the equivalent circuit shown in Fig. 1, which has a light-induced current source, a diode, series resistance, and parallel resistance. These components can have the following relationship between current and voltage [9]:

$$i_{PV} = I_{ph} - I_d \cdot \left[e^{q \cdot \frac{V_{pv} + I \cdot R_s}{\eta \cdot V_T}} - 1 \right] - \frac{V_{pv} + i_{PV} \cdot R_s}{R_p} \quad (1)$$

where I_{ph} is the light-induced current, I_d is the saturation current of the diode, R_s and R_p (which are series and shunt resistance) are parasitic resistance, which is caused by the geometry of the solar cell, and V_T is the thermal voltage. Even though I_d only depends on temperature, I_{ph} is affected by irradiance and temperature, and hence, I_{pv} has a nonlinear function of irradiance, temperature, and V_{pv} [9]. Moreover, since the power of one PV cell is not enough to supply the voltage needed for an industry or a home, a PV cell should be connected in series with a bypass diode. If all the PV cells in a PV module have identical electrical characteristics, the current equation related to the PV module can be represented by

$$i_{pv} = I_{ph} \cdot M - I_d \cdot M \left[e^{q \cdot \frac{V_{tot} + I \cdot R_s}{\eta \cdot V_T \cdot N}} - 1 \right] - \frac{V_{pv} + I_{pv} \cdot R_s}{R_p} \quad (2)$$

where N is the number of cells in series, and M is the number of cells in parallel. V_{tot} is the total voltage from the PV module. The voltage of the PV module is decided by the number of solar cells, while the current is determined by the size of the solar cells. Since a PV module consists of solar cells in series with bypass diodes, the variation in current is not greater than that of the voltage, and is not dependent upon temperature but the tilt angle of the PV module and the shadow of objects. In Fig. 2, the power characteristics of the PV module, which include the situation where one of the PV cells in the PV module is uncovered and covered, are simulated by using data from a solar panel. This curve shows that the PV module is extremely influenced by partial shading.

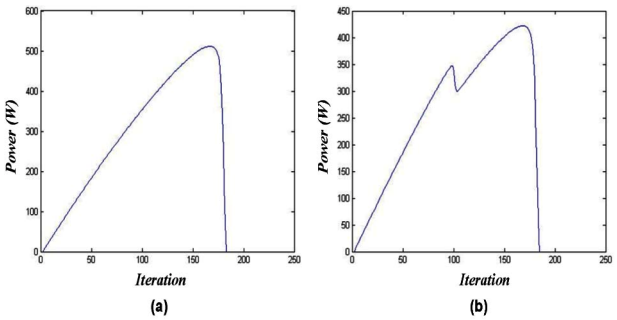

Fig. 2. The equivalent circuit of a photovoltaic cell.

Also, in a real environment, there is a frequent variation of current and voltage in a nearby MPP when using the P&O algorithm and INC. This phenomenon results in reducing the power efficiency of the solar cell panel. The relationship between V_{pv} and I_{pv}, provided that the fluctuation at the maximum operating point is small when compared to MPP, can be shown as follows [3]:

$$i_{PV} = \left.\frac{di_{PV}}{dV_{pv}}\right|_{MPP} \cdot \overline{V_{pv}} + \left.\frac{di_{PV}}{dS}\right|_{MPP} \cdot \overline{S} + \left.\frac{di_{PV}}{dT}\right|_{MPP} \cdot \overline{T} \qquad (3)$$

where symbols with line accent mean small-signal variations in steady-state operation, and S is solar irradiance. If there is constant irradiance, the change in irradiance can be zero. Moreover, since a PV module has high thermal inertia, the variation in temperature can be almost zero. Therefore, (3) represents the following [3]:

$$\begin{aligned} p_{PV} &= P_{PV} + p_{pv} = v_{PV} \cdot i_{PV} \\ &= V_{PV} \cdot I_{PV} + V_{PV} \cdot i_{pv} + v_{pv} \cdot I_{PV} + v_{pv} \cdot i_{pv} \\ &= V_{PV} \cdot I_{PV} - \frac{v_{pv}^{\ 2}}{R_{pv}} \end{aligned} \qquad (4)$$

where V_{PV} and I_{PV} include the fixed value at the MPP and the changing value with a small amount at the MPP. Eq. (4) shows how the available power from a PV module can be reduced when oscillation occurs around the MPP.

As mentioned, partial shading and fluctuation at the MPP can reduce the power efficiency of a PV module. Therefore, in order to increase the power efficiency of the PV module, it is necessary for the MPPT controller to promptly track the MPP and to maintain the MPP without oscillation when weather conditions and the environment around the PV module change. As will be shown in sections 3 and 4, there are two algorithms to track and maintain constant MPP effectively.

3. Description of a Variety of MPPT

In the P&O algorithm, the MPPT controller first measures the input voltage and the current from the PV module. And then, the power calculated by the controller is continually compared with the previous one. Based on the difference between the present one and the previous one, a DC-DC converter changes the input voltage of the PV module by using changed duty from pulse width modulation (PWM). As shown by [3], in order to detect the MPP, all algorithms should know the direction they will move toward. The P&O algorithm can know the correct direction and track the MPP while comparing the present power to the previous one. If present power is more than the previous one, then the P&O algorithm maintains the direction; otherwise, it should be reversed. In this way, the MPP is recognized, and hence, the corresponding voltage in the PV module can be detected. Among MPPT algorithms, P&O has the greatest advantage in terms of easily implementing the system. However, in this algorithm, there are critical disadvantages in a real environment. One of disadvantages is that it is impossible for P&O to track a rapidly changing MPP, such as with broken clouds [10]. This problem can be solved by increasing the perturbation size. However, this solution can also lead to another problem, which is the second disadvantage. Increasing the perturbation size enlarges the range of the oscillation around the MPP, which results in decreasing the power efficiency and the robustness of the components in the MPPT circuit system.

As shown by [8], the flow diagram of the SAR MPPT algorithm includes active mode and power-down mode in the arranged clock period. In active mode, this algorithm can track the MPP with SAR operation with N-bit D_{MPPT}, which can determine the direction of perturbation. Assume that the SAR MPPT algorithm uses 4-bit D_{MPPT}: the starting point for tracking the MPP is at $D_{MPPT} = 1000(\ )$ From the beginning, the SAR MPP algorithm can detect the MPP with half of the previous D_{MPPT} [8]. Since the SAR MPPT algorithm uses binary search instead of a P&O algorithm, which tracks the MPP with a step-by-step system, the time required to detect the MPP is faster than with P&O. If both of them can track the MPP in active mode, P&O and the SAR MPPT require $2^N + 4$ and $2N - 1$ to reach the MPP [8]. In the power-down mode, the SAR MPPT preserves the final value of D_{MPPT} in active mode, and the other operations related to tracking MPP are suspended. By using these techniques, this method can obtain a fast tracking time, and there is no oscillation at the MPP. Nevertheless, there are two serious problems in terms of maintaining and tracking MPP. In Fig. 3, one of them is that the SAR MPPT algorithm always operates with a fixed N-bit D_{MPPT} periodically, which results in checking the MPP with a binary search every active mode cycle, even if the MPP is not changed. It is unnecessary power consumption. Also, if the MPP is changed in power-down mode, this algorithm cannot detect the MPP instantly. Another problem is that there is the probability of not detecting the MPP once in active mode. Since the SAR MPPT algorithm detects the MPP within an arranged N-bit D_{MPPT}, the range that exceeds fixed resolution cannot be found in the first active mode. During this period, unless this algorithm does not find the

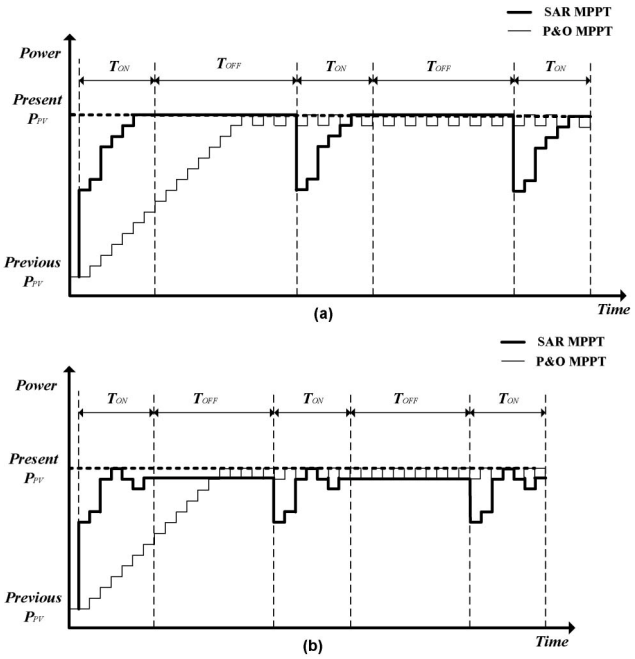

Fig. 3. Comparison graph between P&O and SAR MPPT in two situations where (a) consists of the factor of two, (b) is made by *2N-2*.

MPP, the next active mode will be needed to detect the MPP. This situation takes a longer time than P&O or leads to not tracking the MPP. In Fig. 3(a), the power efficiency of P&O is 59.3%, and that of SAR MPPT is 81.9% until these algorithms finish finding the MPP. However, in Fig. 3(b), the SAR MPPT cannot track the MPP, whereas the power efficiency of P&O is 58.9%.

4. Implementation of the Unbounded Binary Search

Since the maximum power point of solar panels varies according to the environmental conditions, as discussed earlier, the proposed algorithm aims at chasing this optimal working point as fast as possible. This can significantly enhance the power efficiency of a solar panel when the environmental conditions change rapidly.

It also avoids power dissipation by fixing the operating voltage consistently after the MPP is found, instead of continuously perturbing, as the P&O algorithm does. The flowchart illustrating the proposed idea is depicted in Fig. 4 and is meticulously explained in the following. In Fig. 4, the solar panel voltage and current values are sensed and then stored in variables *Vn* and *In*, respectively. The present power is donated by *Pn*, and its value at the

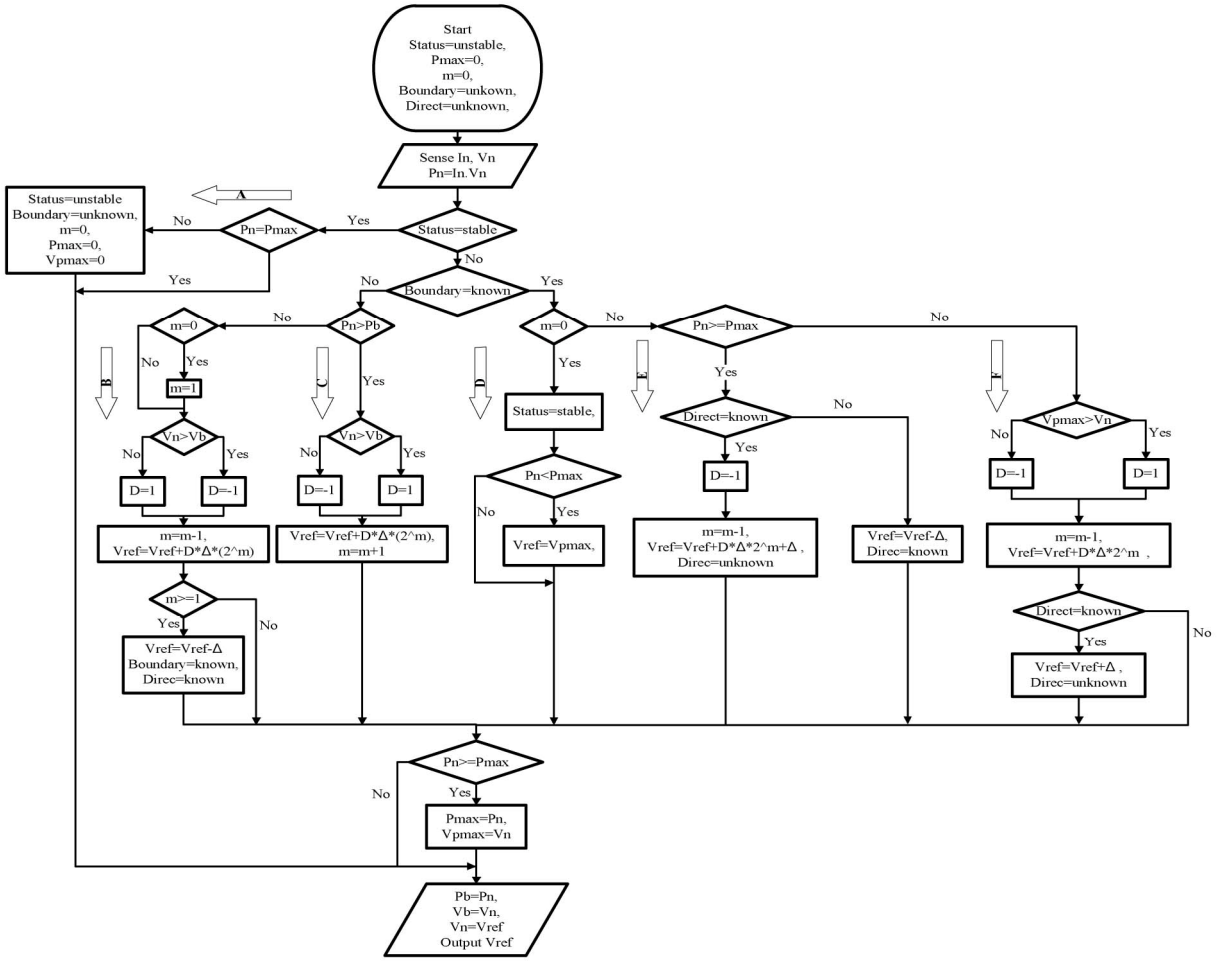

Fig. 4. The flow chart of the UBS algorithm.

previous sampling instant is held by the variable *Pb*. Similarly, *Vb* holds the value of *Vn* in the prior cycle. The maximum power value is donated by *Pmax*, and the voltage that causes the power to be equal to *Pmax* is *Vpmax*. The variable *Status* indicates the stability of the input power. The value of the variable *Boundary* is set to *known* when the algorithm finds the segment of voltage in which the MPP exists.

The index *m* is increased or decreased by one step every cycle to change the duty by a factor of two. When the algorithm operates, it needs to know what direction leads to the MPP. Therefore, the variable *Direc* is used to indicate if the direction is *known* or not. The output of the algorithm is *Vref*, which is the reference output voltage of the solar panel. The operating voltage of the PV panel corresponds to *Vref*.

The operation of the algorithm can be divided into two stages: steady and dynamic. The steady stage means that the MPP is constant, or input power *Pn* is equal to maximum power *Pmax*. In this stage, the algorithm simply continues sensing the input power. And the duty is not changed, as seen in branch (A). When disturbance in the power of the PV panel occurs, the value of the *Status* variable changes to *unstable*. This condition is considered the dynamic stage. The algorithm starts chasing a new maximum power by using the unbounded binary search, setting the variable *Boundary* to *unknown*. For simplicity, let us consider the situation where the maximum power of the PV module moves to a higher voltage, as seen in Fig. 5, where maximum power moving to a lower voltage is similar.

When the MPP is changed, the algorithm at first does not know the direction that the voltage should move to. Therefore, it will make a random movement, which means the voltage will be increased or decreased by one step. This can be done either in branch (B) or branch (C). If this movement makes the power higher, the voltage is constantly altered in the same direction by following branch (C). On the other hand, the changing direction of the voltage is reversed by branch (B). As seen in Fig. 5, the power is enhanced when the voltage increases; therefore, the voltage keeps increasing by a factor of two. Each time the algorithm runs through branch (C), index *m* is increased by 1. In Fig. 5, *m* is increased from 0 to 4. When *m* is 4, the voltage becomes bigger than the MPP voltage. This causes a reduction in the power. The present power, *Pn*, is smaller than the previous power, *Pb*, which is also the temporary maximum power, *Pmax*. Thus, the algorithm operates through branch (C) to reduce the voltage. Note that the voltage is placed at the operating point, which is lower than *Vpmax*, as seen in Step 4 of Fig. 5. This also means that the boundary of the new MPP voltage was already found, so the variable *Boundary* is set to *known*. In the next cycle, present power *Pn* is compared with *Pmax* to determine if the MPP voltage is above or below *Vpmax*. If *Pn* is smaller than *Pmax*, the algorithm follows branch (F). This branch causes the voltage to increase, and index *m* is also reduced by one unit, as seen in Step 5 of Fig. 5. If power *Pn* is bigger than *Pmax*, then the algorithm follows branch (E). However, the algorithm does not know if voltage should be increased or decreased,

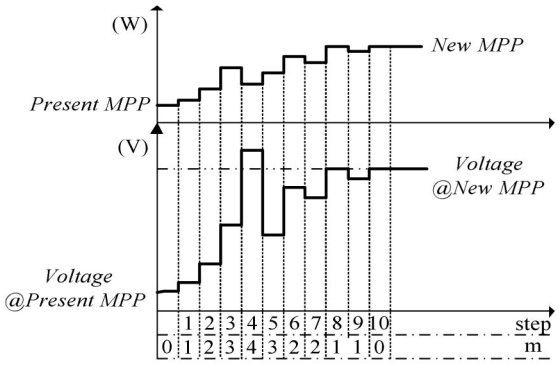

Fig. 5. The MPP tracking procedure of the UBS.

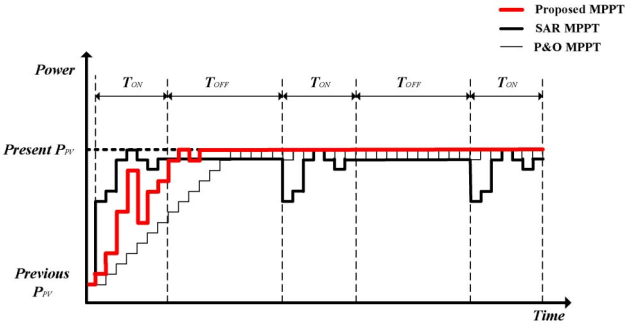

Fig. 6. The comparison of P&O, SAR MPPT, and the UBS.

so it decreases the voltage by one step to check the direction. In Fig. 5, this is illustrated by Step 6. The algorithm keeps running these procedures by branch (E) and branch (F) until index *m* is equal to 0. When m is equal to 0 and branch (D) is followed, the operating voltage is arranged to the MPP voltage. The algorithm stops finding the MPP by setting the variable *Status* to *stable*. Then, it returns to the steady stage. There are some situations determining the worst case when tracking the MPP with the proposed algorithm. Fig. 6 illustrates a comparison among P&O, SAR, and the proposed UBS, and assumes that power is changed with 16 steps. Even if the SAR algorithm uses the binary search to track MPP instantly, this algorithm often cannot track MPP and maintain a constant MPP. This is because the SAR MPPT has a period consisting of active mode and power-down mode. Since this algorithm always starts in active mode, which is periodic, the operating voltage around the MPP moves to find an already arranged MPP. However, this proposed UBS is able to keep the MPP in steady-state operation with binary search, which causes the power efficiency of the PV module to increase. As shown in Fig. 6, the longer the time, the more the proposed UBS can have an advantage in terms of power efficiency. The worst case with the proposed algorithm is at a resolution of four. At the beginning of the MPP tracking procedure, the voltage is changed to the wrong direction, as seen in Step 1 of Fig. 6. The operating voltage is already over the MPP voltage; however, the power is still greater than the previous sampling instant. This makes the voltage change one more step, like Step 6 in Fig. 6. After finding the

boundary of the MPP voltage, the operating voltage moves to the MPP voltage, but the algorithm needs to check the direction every time before changing the voltage. However, in the proposed algorithm, the number of times for direction checking is minimized with the aid of variables *Pmax* and *Dpmax*. The present power is compared with *Pmax* to determine the right direction without the need to check. The practical number for times checking direction is less than the theoretic number of three sampling times. From the discussion above, the total number of chasing steps in the worst case can be calculated by the equation below:

$$3\mathrm{m}+5 \tag{5}$$

where m is the resolution. The total number of chasing steps by the P&O algorithm is

$$2^{m}+4 \tag{6}$$

Fig. 6 is the comparison of chasing step numbers for the proposed algorithm and the conventional algorithm. It is obvious that the proposed algorithm significantly reduces the steps for tracking maximum power point. In Fig. 6, the power efficiency of the proposed UBS is 80.4% and for P&O and SAR MPPT it is 58.9%.

5. Experimental Results

In order to completely evaluate the proposed UBS and compare it with P&O in a real setting, we decided to conduct outdoor field experiments under three kinds of conditions. One of them was an initial condition where the PV panel is fully covered and then uncovered. The second was with one screened PV cell. The last was with one uncovered PV cell and one covered PV cell. The conditions, instead of the initial condition, are the worst conditions for the proposed algorithm. Since the variation of voltage is too small when shading one PV cell of the PV module, P&O could perform better than the proposed algorithm. Therefore, the smallest variation can occur when we cover just one cell of the PV panel. This paper already suggested the optimal resolution of the proposed UBS in the principle way, and will demonstrate a reasonable resolution by using the data from the real setting. The PV panel (JSM100-36-01, Sunk-Kyung Tech.) was mounted on the rooftop of the engineering college in Chung-Ang University while maintaining a position perpendicular to the sun. This PV panel has $V_{mp}=17.636V$ and $I_{mp}=5.697A$ at $1000\mathrm{kW}/m^2$ and $25℃$. At the time this work was conducted, they were $V_{mp}=15.38V$ and $I_{mp}=4.45A$ at $1000\mathrm{kW}/m^2$ and $20℃$. The MPPT system consists of a boost converter with an MCU and 6 ohm load resistors. Also, there is equipment to measure solar irradiance. To analyze the data from the MPPT system, an Agilent oscilloscope (MSO 6052) and a monitoring program made for this work were used. This monitoring program has a function to measure the

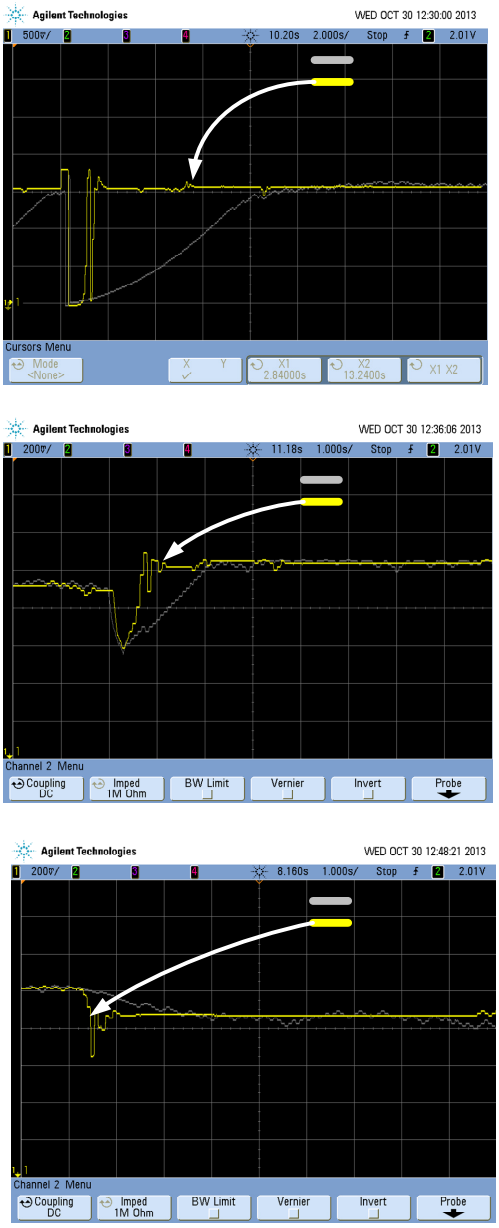

Fig. 7. The measured result of the UBS at (a) the initial condition, (b) the condition where one PV cell in the PV module is covered, (c) the condition where one PV cell is covered and then uncovered with a 7-bit MPPT.

input/output voltages, the current, the duty of the PWM and power. Fig. 9 shows a photograph of the field setup. The PV panel was connected to the MPPT system, which provided the data to a laptop and oscilloscope through serial port communications and SMA cables. This field measurement operated with one PV panel on a clear day. The time for inputting the codes for P&O and the UBS algorithm was less than 10s. Therefore, the variation in MPP when changing codes can be considered negligible. As shown in Fig. 7, under three kinds of condition, the proposed 7-bit UBS is faster by 87.3%, 60% and 66.1% compared to 7-bit P&O. Thus, these data, measured in an outdoor test site, verify that the proposed UBS is slower

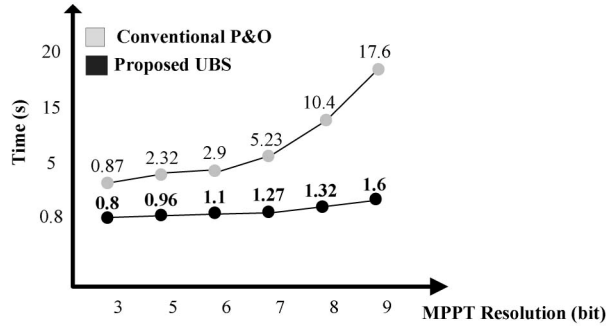

Fig. 8. The measured time according to duty resolution (MPPT resolution).

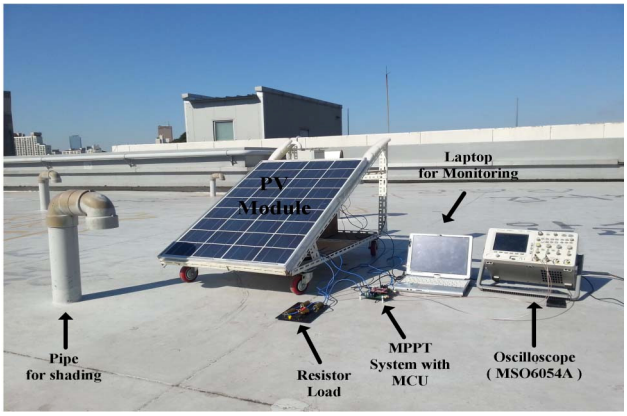

Fig. 9. Test environment.

than P&O when operated below 3-bit. The power efficiency of each 7-bit algorithm was measured in dynamic-state operation and in steady-state operation for 20 s. The proposed UBS can always obtain higher power efficiency than P&O in dynamic-state operation due to the binary search. In steady-state operation, the proposed UBS is more efficient than P&O. This is because this proposed algorithm fixes the voltage to the MPP until a new MPP is detected by the proposed USB, instead of the operating voltage continuously moving around the MPP. Therefore, the proposed algorithm is superior to P&O in both operating states. And by using the proposed UBS, this work can obtain power efficiency of 97.52% and 98.12% in dynamic-state operation and steady-state operation, respectively.

6. Conclusion

This paper presents a proposed MPPT algorithm and system for a PV panel, which is able to obtain the MPP with fast tracking time and no oscillation around the MPP. Since the algorithm uses unbounded binary search, the variation in operating voltage due to rapid weather change is easily detected. After finding the voltage at the MPP, it is possible for the voltage to be fixed by using the proposed algorithm. The margin for maintaining maximum power can pose a problem for the accuracy of the MPP. However, this work already assigned the margin below the minimum range of fluctuation from P&O under steady-state operation. Given three kinds of conditions, the proposed UBS evens the advantages in terms of tracking response time and oscillation in the worst-case scenario, where one cell in the PV module is covered. The proposed method was implemented and compared with P&O. The experimental results verified which algorithm is better for response time and power efficiency. Thus, the proposed UBS is applicable to controlling a PV module in a real environment.

Acknowledgement

This research was supported by the Basic Science Research Program through the National Research Foundation of Korea (NRF) funded by the Ministry of Education (No. 2015R1D1A1A01060031) and was also supported by the IT R&D program of MOTIE/KEIT. [10054819, Development of modular wearable platform technology for the disaster and industrial site].

References

[1] Y.-S. Kim, and R. Winston, "Unbounded Binary Search for a Fast and an Accurate Maximum Power point Tracking, " *7th Int. Conf. on Concentrating Photo. Systems.,* Proc. 1407, pp. 289-292, 2011.

[2] S. Liu, and R.A. Dougal, "Dynamic multiphysics model for solar array," *IEEE Trans. Energy Conv.*, vol. 17, no. 2, pp.285-294, Jun. 2002.

[3] N. Femia, G. Petrone, G. Spagnuolo, and M. Vitelli, "Optimization of perturb and observe maximum power point tracking method," *IEEE Trans. Power Electron.*, vol. 20, no. 4, pp. 963–973, Jul. 2005.

[4] F. Harashima, H. Inaba, S. Kondo, and N. Takashima, Chen, "Microprocessor-Controlled SIT Inverter for Solar Energy System," *IEEE Trans. Ind. Electron.*, vol. IE-34, no. 1, pp.50-55, Feb. 1987.

[5] D. Sera, R. Teodorescu, J. Hantschel, and M. Knoll, "Optimized- Maximum Power Point Tracker for Fast-Changing Environmental Conditions," *IEEE Trans. Ind. Electron.*, vol. 55, no. 7, pp.2629-2637, Jul. 2008.

[6] Y.C. Kuo, T.J. Liang, and J.F. Chen, "Novel maximum-power-point-tracking controller for photovoltaic," *IEEE Trans. Ind. Electron.*, vol. 48, no. 3, pp. 594–601, Jun. 2001.

[7] G. Hsieh, H. Hsieh, C. Tasai, and C.Wang, "Photovoltaic Power-Increment-Aided Incremental-Conductance MPPT with Two-Phased Tracking," *IEEE Trans. Power Electron.*, vol. 28, no. 6, pp. 2895–2911, Jun. 2013.

[8] H.-K. Kim, S.-J. Kim, C.-K. Kwon, Y.-J. Min, C.-W. Kim, and S.-W. Kim, "An Energy-Efficient Fast Maximum Power Point Tracking Circuit in an 800-*u*W Photovoltaic Energy Harvester," *IEEE Trans. Power Electron.*, vol. 28, no. 6, pp. 2927–2935, Jun. 2013.

[9] Y.-S. Kim, S.-M Kang, and R. Winston, "Modeling of a concentrating photovoltaic system for optimum

land use," *Progress in Photovoltaics: Research and Applications*., vol. 21, issue. 2, pp. 240-249, Mar. 2013.
[10] P. Robert C. N., and P. David J., "Sub-module Integrated Distributed Maximum Power Point Tracking for Solar Photovoltaic Applications," *IEEE Trans. Power Electron.*, vol. 28, no. 6, pp. 2957–2967, Jun. 2013.
[11] "Trends in photovoltaic applications. Survey report of selected IEA countries between 1992 and 2006," Int. Energy Agency Photovoltaic Power Syst., Paris, France, Tech. Rep. IEA-PVPS T1-16:2007, 2007 [Online]. Available at Article (CrossRef Link)
[12] B. Subudhi, and R. Pradhan, "A Comparative Study on Maximum Power Point Tracking Techniques for Photovoltaic Power Systems, *IEEE Trans. Sustainable Energy*., vol. 4, pp. 89-98, Jan. 2013.

Yohan Hong received a BSc and an MSc in electrical and electronics engineering from Chung-Ang University, Seoul, Korea, in 2010 and 2014, respectively, and is currently working toward a PhD in electrical and electronics engineering at Chung-Ang University. Since 2010, he has been involved with the development of a front-end system including LNA and ADC. Currently, his research interests are maximum power point tracking algorithms for a distributed PV system, and pipeline ADC.

Yong Sin Kim received a BSc and an MSc in Electronics from Korea University, Seoul, Korea, in 1999 and 2003, respectively. He obtained his PhD in Electrical Engineering from the University of California at Santa Cruz, USA, in 2008. From 2008 to 2012, he worked at the University of California Advanced Solar Technologies Institute (UC Solar), where he researched optimizing power in distributed photovoltaic systems. From 2012 to 2014, he was with School of Electrical and Electronics Engineering, Chung-Ang University, Seoul, Korea, where he was involved in development of sensors for human–machine interfaces. Since March 2014, he has been with School of Electrical Engineering, Korea University, Seoul, Korea. His current research interests include cross-disciplinary integration of circuits and systems for energy harvesting and sensor applications.

Kwang-Hyun Baek received his BSc and MSc from Korea University, Seoul, Korea, and a PhD in electrical engineering from the University of Illinois at Urbana-Champaign, IL, USA, in 2002. From 1990 to 1996, he was with Samsung Electronics, and he was with the Department of High-Speed Mixed-Signal ICs as a senior scientist at Rockwell Scientific Company, formerly Rockwell Science Center (RSC), Thousand Oaks, CA, USA, from 2000 to 2006. At RSC, he was involved in development of high-speed data converters (ADC/DAC) and direct digital frequency synthesizers (DDFS). Since 2006, he has been with the School of Electrical and Electronics Engineering, Chung-Ang University, Seoul, Korea, where he is a faculty member. His research interests include high-performance analog and digital integrated-circuit design, modeling, and synthesis.